PROCEEDINGS OF THE ROYAL SOCIETY A

rspa.royalsocietypublishing.org

Research

Cite this article: Kausel E. 2013 Lamb's problem at its simplest. Proc R Soc A 469: 20120462.
http://dx.doi.org/10.1098/rspa.2012.0462

Received: 2 August 2012
Accepted: 19 September 2012

Subject Areas:
geophysics, wave motion, mechanics

Keywords:
Lamb's problem, Green's functions, seismology, soil dynamics, earthquake engineering, wave motion

Author for correspondence:
Eduardo Kausel
e-mail: kausel@mit.edu

Electronic supplementary material is available at http://dx.doi.org/10.1098/rspa.2012.0462 or via http://rspa.royalsocietypublishing.org.

Royal Society Publishing
Informing the science of the future

Lamb's problem at its simplest

Eduardo Kausel

Civil and Environmental Engineering, Massachusetts Institute of Technology, Cambridge, MA 02139, USA

This article revisits the classical problem of horizontal and vertical point loads suddenly applied onto the surface of a homogeneous, elastic half-space, and provides a complete set of exact, explicit formulae which are cast in the most compact format and with the simplest possible structure. The formulae given are valid for the full range of Poisson's ratios from 0 to 0.5, and they treat real and complex poles alike, as a result of which a single set of formulae suffices and also exact formulae for dipoles can be given.

1. Introduction

Lamb's problem deals with the response elicited by a vertical or horizontal point load applied suddenly onto the surface of an elastic half-space. This classical problem harks back to the early twentieth century, when Lamb [1] enunciated this now famous and emblematic problem in seismology.

The first truly complete solutions to Lamb's problem were given by Pekeris [2] and Chao [3], who provided closed-form expressions for the components of motion elicited by a vertical and a horizontal load, respectively, but only when Poisson's ratio is 1/4. This problem was taken up again by Mooney [4], who extended the Pekeris solution to any arbitrary Poisson's ratio, but he did so only for the vertical component while ignoring the radial one. Then in 1979, Richards considered this problem once again and gave a complete set of exact formulae for both loading cases and for any Poisson's ratio in a paper that has remained largely unknown within the elastodynamics and wave propagation communities. Part of the reason may have been that Richards only presented the final formulae in the context of a note on spontaneous crack propagation without indicating where their rather complicated derivation could be found. Also, he did not summarize these in his book [5], perhaps because he judged these to be unimportant. This seems to be corroborated by two comments in his brief article, namely '*these formulas would be only a minor curiosity*', and '*Perhaps the main achievement of this paper* ... ', as if he were unsure of their true worth.

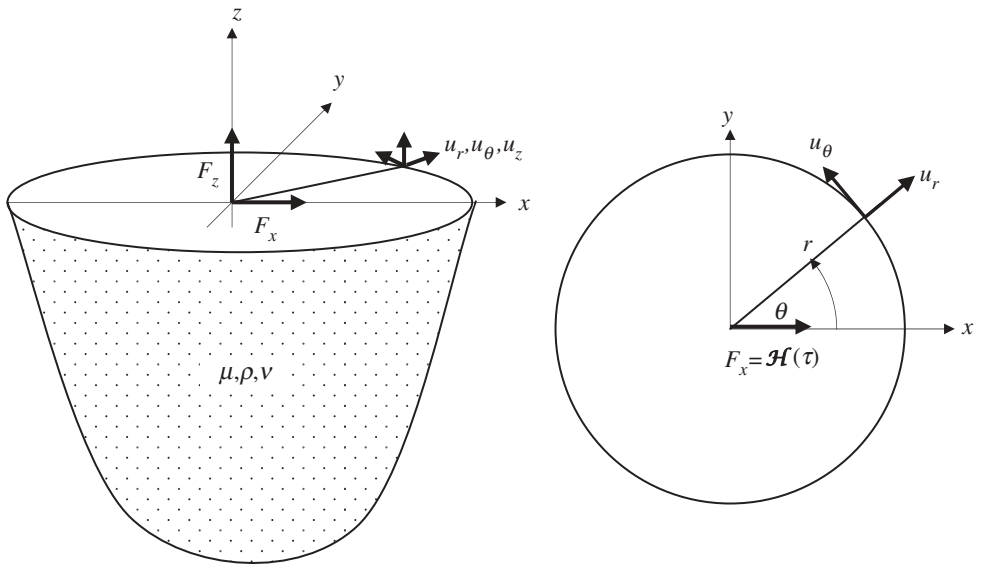

Figure 1. System of coordinates.

It is the purpose of this technical note to present a new rendition of Lamb's problem by means of a very compact set of exact formulae for all loading cases and for any Poisson's ratio which are fully equivalent to, but much simpler than Richards'. In a nutshell, the formulae are obtained by casting the equations of motion in the Laplace-radial wavenumber domain (s, k), carrying out an inverse Laplace transform into the time domain by a contour integration based on a generalization of the so-called Bateman–Pekeris theorem, followed by Hankel transforms evaluated with the aid of Mooney's integral together with an expansion of the integrand into partial fractions. Although the formulae herein are listed without proof, their complete derivation can be found in the electronic supplementary material.

The ensuing provides the complete set of formulae in Lamb's problem cast in a consistent, right-handed, upright coordinate system, and which is valid for the full range of Poisson's ratios from 0 to 0.5. We bring about a significant organization and simplification to the formulae by reducing the number as well as the form of the constants involved, and most importantly, by providing expressions which make no distinction between a real or complex root, a feature that provides for a seamless transition into the complex domain and greatly simplifies the task of taking derivatives. This also allows us to provide simple, explicit expressions for a subset of Lamb dipoles.

2. Notation and definitions

Consider a lower, homogeneous elastic half-space $z \leq 0$ onto whose upper surface $z = 0$ we suddenly apply either an upright vertical or a horizontal-x (tangential) point force of unit intensity which remains constant thereafter. Thus, the force has the time dependence of a step function $\mathcal{H}(\tau)$ i.e. a Heaviside function. A right-handed, cylindrical coordinate system r, θ, z with the origin at the location of the force on the surface is used throughout, i.e. the vertical force and vertical displacements are both positive up, while the horizontal force acts in the positive x-direction (i.e. radial direction with $\theta = 0$), see figure 1.

The following symbols are used in the ensuing:

r radial distance (range)

θ azimuth

μ shear modulus

ρ mass density
ν Poisson's ratio
C_R Rayleigh wave velocity
C_S shear wave velocity
C_P pressure wave velocity
t time
a $= C_S/C_P =$ ratio of S to P wave velocity
κ_j $= C_S/C_j =$ three dimensionless solutions to the Rayleigh characteristic equation
γ $\equiv \kappa_1 = C_S/C_R =$ true Rayleigh root
τ $= tC_S/r =$ dimensionless time.

In a nutshell, the application of the formulae requires the straightforward task of finding the three roots $\kappa_1^2, \kappa_2^2, \kappa_3^2$ of the rationalized, bi-cubic Rayleigh function

$$16(1-a^2)\kappa^6 - 8(3-2a^2)\kappa^4 + 8\kappa^2 - 1 = 0, \tag{2.1}$$

of which the first one is the real, true Rayleigh root and the remaining two are the non-physical roots. At low Poisson's ratio the latter two are real-valued, but they turn complex when Poisson's ratio exceeds the threshold $\nu > 0.2631$. Associated with each of the three roots κ_j, where $j = 1, 2, 3$, we define the three sets of coefficients as follows:

$$A_j = \frac{(\kappa_j^2 - \frac{1}{2})^2\sqrt{a^2-\kappa_j^2}}{D_j}, \quad B_j = \frac{(1-2\kappa_j^2)(1-\kappa_j^2)}{D_j}, \quad C_j = \frac{(1-\kappa_j^2)\sqrt{a^2-\kappa_j^2}}{D_j} \tag{2.2a}$$

and

$$D_j = (\kappa_j^2 - \kappa_i^2)(\kappa_j^2 - \kappa_k^2), \quad i \neq j \neq k. \tag{2.2b}$$

These coefficients, which can be real or complex, will be used in the response functions given in §4. Observe that the two indices in i and k in equation (2.2*b*) are inferred from j by cyclic order. For example, $j = 1$ implies $i = 2$ and $k = 3$ (or what is exactly the same, $i = 3, k = 2$), and so forth. Thus, allowable triplets are $(i, j, k) = (1, 2, 3), (2, 3, 1), (3, 1, 2)$.

3. Preliminary comment on square root terms in the formulae

As can be seen, the coefficients A_j and C_j given by equation (2.2) contain square root terms in the three roots of equation (2.1). In a practical implementation of the formulae listed in the ensuing and for the true Rayleigh root $\kappa_1 \equiv \gamma > 1$ and for $\tau < \gamma$, it might seem preferable to define the real, transformed coefficients

$$\bar{A}_1 = \frac{(\gamma^2 - \frac{1}{2})^2\sqrt{\gamma^2-a^2}}{(\gamma^2-\kappa_2^2)(\gamma^2-\kappa_3^2)} \quad \text{and} \quad \bar{C}_1 = \frac{(1-\gamma^2)\sqrt{\gamma^2-a^2}}{(\gamma^2-\kappa_2^2)(\gamma^2-\kappa_3^2)},$$

such that for $\tau < \gamma$

$$\frac{A_1}{\sqrt{\tau^2-\gamma^2}} = \frac{\bar{A}_1}{\sqrt{\gamma^2-\tau^2}}, \quad \frac{C_1}{\sqrt{\tau^2-\gamma^2}} = \frac{\bar{C}_1}{\sqrt{\gamma^2-\tau^2}}, \quad C_1\sqrt{\tau^2-\gamma^2} = (-)\bar{C}_1\sqrt{\gamma^2-\tau^2},$$

all of which follow readily from the transformations

$$\frac{\sqrt{a^2-\kappa_1^2}}{\sqrt{\tau^2-\kappa_1^2}} \equiv \frac{\sqrt{a^2-\gamma^2}}{\sqrt{\tau^2-\gamma^2}} = \frac{\mathrm{i}\sqrt{\gamma^2-a^2}}{\mathrm{i}\sqrt{\gamma^2-\tau^2}} = \frac{\sqrt{\gamma^2-a^2}}{\sqrt{\gamma^2-\tau^2}}$$

and

$$\sqrt{a^2-\kappa_1^2}\sqrt{\tau^2-\kappa_1^2} \equiv \sqrt{a^2-\gamma^2}\sqrt{\tau^2-\gamma^2} = \left(\mathrm{i}\sqrt{\gamma^2-a^2}\right)\left(\mathrm{i}\sqrt{\gamma^2-\tau^2}\right)$$
$$= (-)\sqrt{\gamma^2-a^2}\sqrt{\gamma^2-\tau^2}$$

(note: use of $-\mathrm{i}$ instead of $+\mathrm{i}$ leads to the same result, because the negative sign cancels out in either the product or division).

Although we could indeed express our response functions in terms of a mixed set of coefficients $\bar{A}_1, A_2, A_3$ and $\bar{C}_1, C_2, C_3$, we prefer to use the definitions given by equation (2.2) throughout for the following reasons.

— Fewer constants are needed for the response functions, which allows adding terms via summation signs. This facilitates and simplifies in turn the derivation and presentation of the formulae for the dipoles.
— The resulting formulae are then largely independent of the numbering sequence used for the roots, so these could be renumbered according to user preference or programming environment. Also, any leading negative signs, such as the one above, now arise naturally from the formulation itself, which thus avoids ad hoc sign reversals that depend on the numbering sequence.
— The same spatio-temporal differentiation rules apply to all roots, see §§8 and 10.
— Most importantly, our formulae are then *universal*, that is, they are valid no matter what Poisson's ratio may be, and whether or not the false roots are real or appear in complex-conjugate pairs.

Of course, when implementing the formulae into a computer program, users can readily make use of the aforementioned transformations to avoid the complex algebra for the term contributed by the Rayleigh root. Similarly, when the roots appear in complex-conjugate pairs, one could also replace their contribution to a summation by doubling the real part of one of these. However, these are merely implementation issues that will be sidestepped herein and left to the readers to sort out.

4. Response functions

With reference to figure 1, the response functions are the following (their derivation can be found in the electronic supplementary material):

(a) Vertical displacement owing to vertical load

$$u_{zz}(r,\tau) = \frac{(1-\nu)}{2\pi\mu r}\begin{cases} \dfrac{1}{2}\left(1 - \displaystyle\sum_{j=1}^{3} \frac{A_j}{\sqrt{\tau^2-\kappa_j^2}}\right), & a < \tau < 1, \\ 1 - \dfrac{A_1}{\sqrt{\tau^2-\gamma^2}}, & 1 \le \tau < \gamma, \\ 1, & \tau \ge \gamma. \end{cases} \tag{4.1}$$

(b) Radial displacement owing to horizontal load

$$u_{rx} = \frac{(\cos\theta)}{2\pi\mu r}\begin{cases} \dfrac{1}{2}(1-\nu)\tau^2 \displaystyle\sum_{j=1}^{3} \frac{C_j}{\sqrt{\tau^2-\kappa_j^2}}, & a < \tau < 1, \\ 1 + (1-\nu)\tau^2 \dfrac{C_1}{\sqrt{\tau^2-r^2}}, & 1 \le \tau < \gamma, \\ 1, & \tau \ge \gamma. \end{cases} \tag{4.2}$$

(c) Tangential displacement owing to horizontal load

$$u_{\theta x} = \frac{(1-\nu)(-\sin\theta)}{2\pi\mu r}\begin{cases}\dfrac{1}{2}\left[1-\displaystyle\sum_{j=1}^{3} C_j\sqrt{\tau^2-\kappa_j^2}\right], & a<\tau<1,\\ 1-C_1\sqrt{\tau^2-\gamma^2}, & 1\le\tau<\gamma\\ 1, & \tau\ge\gamma.\end{cases} \tag{4.3}$$

(d) Radial displacement owing to a vertical load

$$u_{rz}(r,\tau) = \frac{\tau}{8\pi\mu r}\begin{cases}\dfrac{1}{\pi(1-a^2)^{3/2}}\left\{2K(n)-\displaystyle\sum_{j=1}^{3} B_j\Pi(n^2 m_j,n)\right\}, & a<\tau<1,\\ \dfrac{n^{-1}}{\pi(1-a^2)^{3/2}}\left\{2K(n^{-1})-\displaystyle\sum_{j=1}^{3} B_j\Pi(m_j,n^{-1})\right\}, & 1\le\tau<\gamma,\\ \dfrac{n^{-1}}{\pi(1-a^2)^{3/2}}\left\{2K(n^{-1})-\displaystyle\sum_{j=1}^{3} B_j\Pi(m_j,n^{-1})\right\}+\dfrac{2}{\sqrt{\tau^2-\gamma^2}}D, & \tau\ge\gamma,\end{cases} \tag{4.4}$$

where

$$n^2=\frac{\tau^2-a^2}{1-a^2},\quad m_j=\frac{1-a^2}{a^2-\kappa_j^2},\quad D=\frac{(2\gamma^2-1)^3}{8(1-a^2)\gamma^6-4\gamma^2+1}. \tag{4.5}$$

In these expressions,

$$K(n)=\int_0^{(1/2)\pi}\frac{\mathrm{d}\theta}{\sqrt{1-n^2\sin^2\theta}}\quad\text{and}\quad \Pi(m,n)=\int_0^{(1/2)\pi}\frac{\mathrm{d}\theta}{(1+m\sin^2\theta)\sqrt{1-n^2\sin^2\theta}} \tag{4.6}$$

are the complete elliptic functions of the first and third kind, respectively. In the case of complex roots, the characteristic m turns complex, in which case the elliptic Π function satisfies the complex-conjugate symmetry $\Pi(m^*,n)=\Pi^*(m,n)$. To the best of the author's knowledge and as of this writing, only Mathematica—but not Maple or Matlab—seems to provide the capability of complex characteristic. However, it is not difficult to implement effective numerical routines which allow for complex values of these parameters (one such routine is available in the electronic supplementary material).

(e) Vertical displacement owing to horizontal load

Because of the reciprocity principle, the vertical displacement elicited by a horizontal load is numerically equal to the horizontal (radial) displacement due to a vertical load, except for a sign change and also for the fact that it varies with the cosine of the azimuth

$$u_{zx}(r,\theta,\tau)=-u_{rz}(r,\tau)\cos\theta.$$

5. Displacements at depth along the epicentral axis

At $r=0$ and a depth $d=|z|$, the displacements at dimensionless time $\tau=tC_S/|z|$ are

$$u_{xx}=\frac{1}{4\pi\mu|z|}[f_S(\tau)\mathcal{H}(\tau-1)-f_P(\tau)\mathcal{H}(\tau-a)] \tag{5.1a}$$

and

$$u_{zz} = \frac{1}{2\pi\mu|z|}[g_{\mathrm{P}}(\tau)\mathcal{H}(\tau - a) - g_{\mathrm{S}}(\tau)\mathcal{H}(\tau - 1)], \tag{5.1b}$$

where

$$f_{\mathrm{P}} = \frac{2\tau(\tau^2 - a^2)S_1}{(2\tau^2 - 2a^2 + 1)^2 - 4\tau(\tau^2 - a^2)S_1}, \quad f_{\mathrm{S}} = 1 + \frac{(2\tau^2 - 1)\tau^2}{(2\tau^2 - 1)^2 - 4\tau(\tau^2 - 1)S_2} \tag{5.2a}$$

$$g_{\mathrm{P}} = \frac{\tau^2(2\tau^2 - 2a^2 + 1)}{(2\tau^2 - 2a^2 + 1)^2 - 4\tau(\tau^2 - a^2)S_1}, \quad g_{\mathrm{S}} = \frac{2\tau(\tau^2 - 1)S_2}{(2\tau^2 - 1)^2 - 4\tau(\tau^2 - 1)S_2} \tag{5.2b}$$

and

$$S_1 = \sqrt{\tau^2 + 1 - a^2}, \quad S_2 = \sqrt{\tau^2 - 1 + a^2}. \tag{5.2c}$$

Although simple in appearance, at large times $\tau \gg 1$ the above representation suffers from severe cancellations. The reason is that although the sum of the two functions tends to a constant (static) value, individually each function grows without bound with time. This problem can be avoided by means of the following fully equivalent formulae for $\tau > 1$:

$$u_{xx} = \frac{1}{4\pi\mu|z|}\left\{1 - (1 - a^2)\left[\frac{(\tau^2 - a^2)(2\tau^2 - 2a^2 + 1)^2}{\frac{1}{2}(1 + S_1/\tau)D_1} + \frac{2\tau^2(2\tau^2 - 1)(\tau^2 - 1)}{\frac{1}{2}(1 + S_2/\tau)D_2}\right] + \frac{1}{D_1 D_2}\sum_{j=2,4,}^{12} a_j\tau^j\right\} \tag{5.3a}$$

and

$$u_{zz} = \frac{1}{2\pi\mu|z|}\left\{(1 - a^2)\left[\frac{2\tau^2(2\tau^2 - 2a^2 + 1)(\tau^2 - a^2)}{\frac{1}{2}(S_1/\tau + 1)D_1} + \frac{(\tau^2 - 1)(2\tau^2 - 1)^2}{\frac{1}{2}(S_2/\tau + 1)D_2}\right] + \frac{1}{D_1 D_2}\sum_{j=2,4,}^{12} b_j\tau^j\right\}, \tag{5.3b}$$

where

$$D_1 = 16(1 - a^2)\tau^6 + 8(6a^4 - 8a^2 + 3)\tau^4 - 8(6a^6 - 10a^4 + 6a^2 - 1)\tau^2 + (1 - 2a^2)^4 \tag{5.4a}$$

and

$$D_2 = 16(1 - a^2)\tau^6 - 8(3 - 4a^2)\tau^4 + 8(1 - 2a^2)\tau^2 + 1, \tag{5.4b}$$

and the coefficients of the two summations (obtained with Matlab's symbolic tool) are

$$\left.\begin{aligned} a_{12} &= 128(1 - a^2), \\ a_{10} &= -64(1 + 4a^2 - 6a^4), \\ a_8 &= -16(3 - 15a^2 - 4a^4 + 24a^6), \\ a_6 &= 16a^2(4 - 17a^2 + 10a^4 + 8a^6), \\ a_4 &= 16a^2(1 - 3a^2 + 7a^4 - 6a^6), \\ a_2 &= -(1 - 10a^2 + 40a^4 - 48a^6 + 16a^8) \end{aligned}\right\} \tag{5.5a}$$

and

$$\left.\begin{aligned} b_{12} &= 128(1 - a^2), \\ b_{10} &= 64(1 - 2a^2)(2 - 4a^2 + a^4), \\ b_8 &= -16(21 - 37a^2 + 4a^4 + 36a^6 - 16a^8), \\ b_6 &= 16(3 + 26a^2 - 78a^4 + 70a^6 - 8a^8 - 8a^{10}), \\ b_4 &= 4(15 - 87a^2 + 116a^4 + 24a^6 - 136a^8 + 64a^{10}), \\ b_2 &= (11 - 28a^2 + 16a^4)(1 - 2a^2)^3. \end{aligned}\right\} \tag{5.5b}$$

At large times, the above converge to

$$D_1 = D_2 \to 16(1 - a^2)\tau^6 + \cdots, \quad \Sigma \to a_{12}\tau^{12} + \cdots, \quad \frac{1}{2}\left(1 + \frac{S_j}{\tau}\right) \to 1,$$

so,

$$u_{xx} \to \frac{1}{4\pi\mu|z|}\left\{1 - \frac{(1-a^2)8}{16(1-a^2)} + \frac{128(1-a^2)}{16^2(1-a^2)^2}\right\} = \frac{1}{8\pi\mu|z|}\frac{2-a^2}{(1-a^2)} = \frac{3-2\nu}{8\pi\mu|z|} \tag{5.6a}$$

and

$$u_{zz} \to \frac{1}{4\pi\mu|z|}\left(\frac{2-a^2}{1-a^2}\right) = \frac{3-2\nu}{4\pi\mu|z|}, \tag{5.6b}$$

which are the correct limits predicted by the Cerruti and Boussinesq [6,7] theories for static tangential and vertical loads applied onto the surface of a half-space.

6. Discontinuities and singularities

(a) Arrival of P wave, $\tau = a$

At the arrival of the P wave, all response functions at the surface are continuous, even if their slopes are not. Still, all temporal derivatives are zero at $\tau = a^-$ while shortly thereafter at $\tau = a^+$, they are well defined.

On the other hand, of the two response functions at depth on the epicentral axis, the response due to a vertical load exhibits a jump of magnitude

$$\Delta u_{zz}|_{\tau=a} = \frac{a^2}{2\pi\mu|z|} = \frac{1-2\nu}{4(1-\nu)\pi\mu|z|}, \tag{6.1}$$

which is properly accounted to by the Heaviside term $\mathcal{H}(\tau - a)$ in equation (5.1*b*), so the singularity in the temporal derivative will arise naturally from the differentiation of that step function.

(b) Arrival of S wave, $\tau = 1$

All but one of the response functions—but not their slopes—are continuous at the surface. The notable exception is the tangential displacement owing to a horizontal load (equation (4.3)), which is discontinuous at that location. Analysing equation (4.3) with Matlab's symbolic tool, this discontinuity can be shown to be given by

$$\begin{aligned}\Delta u_{\theta x}|_{\tau=1} &= \frac{(1-\nu)}{4\pi\mu r}(-\sin\theta)\left\{1 - C_1\sqrt{1-\kappa_1^2} + C_2\sqrt{1-\kappa_2^2} + C_3\sqrt{1-\kappa_3^2}\right\} \\ &= \frac{1}{2\pi\mu r}(-\sin\theta).\end{aligned} \tag{6.2}$$

Observe the remarkable fact that the jump is ultimately independent of Poisson's ratio, even though the function itself depends on that ratio at all other times. This shows that the discontinuity is caused by the arrival of an SH wave. Furthermore, the jump implies that the temporal derivative (i.e. with respect to τ) will exhibit a singularity

$$\frac{\delta(\tau-1)}{2\pi\mu r}(-\sin\theta), \tag{6.3}$$

which must be accounted for when the temporal derivatives are obtained by direct differentiation at $\tau = 1^-$ and $\tau = 1^+$, i.e. in the case of the dipoles considered later on.

At points below the surface along the epicentral axis, the horizontal displacement is discontinuous, and the jump is

$$\Delta u_{xx}|_{\tau=1} = \frac{1}{2\pi\mu|z|}, \tag{6.4}$$

but again this discontinuity is properly accounted for by the Heaviside term $\mathcal{H}(\tau - 1)$ which will contribute properly to the singularity of the slope at this point in time.

(c) Arrival of R wave, $\tau = \gamma$

The functions in u_{zz} and u_{rx} (equations (4.1) and (4.2)) exhibit an integrable, negative-valued singularity in the neighbourhood $\tau = \gamma^-$. Immediately thereafter, following the passage of the Rayleigh wave, these response functions jump to their final, positive, static values at $\tau = \gamma^+$, i.e.

$$\Delta u_{zz}|_{\tau=\gamma} = \frac{1-\nu}{2\pi\mu r}, \quad \Delta u_{rx}|_{\tau=\gamma} = \frac{(\cos\theta)}{2\pi\mu r}. \tag{6.5}$$

Thus, when differentiated with respect to time, these jumps will add a positive singularity immediately following the negative singularity, i.e.

$$\frac{1-\nu}{2\pi\mu r}\delta(\tau-\gamma) \quad \text{and} \quad \frac{(\cos\theta)}{2\pi\mu r}\delta(\tau-\gamma), \tag{6.6}$$

respectively. These must be accounted for when computing velocities, dipoles, or the response function owing to impulsive loads.

On the other hand, the displacement functions u_{rz} and u_{zx} also exhibit an integrable singularity at $\tau = \gamma^+$—because of the term in D in equation (4.4)—but are otherwise continuous.

7. Transformation into cartesian coordinates

The displacement functions in all of the formulae in equations (4.1)–(4.4) can be cast in terms of cylindrical amplitudes $\tilde{u}_{\ell r}, \tilde{u}_{\ell\theta}, \tilde{u}_{\ell z}$ by writing the response functions in the form

$$u_r = \tilde{u}_{\ell r}(\cos\ell\theta), \quad u_\theta = \tilde{u}_{\ell\theta}(-\sin\ell\theta) \quad u_z = \tilde{u}_{\ell z}(\cos\ell\theta), \tag{7.1}$$

where $\ell = 0$ for the vertical load, and $\ell = 1$ for the horizontal load. These amplitudes are closely related to the integrals $I_1, \ldots, I_4$ in Richards [8]. The Cartesian components of the displacement vector are then given by

$$u_x = \tilde{u}_{\ell r}\cos\ell\theta\cos\theta + \tilde{u}_{\ell\theta}\sin\ell\theta\sin\theta, \tag{7.2a}$$

$$u_y = \tilde{u}_{\ell r}\cos\ell\theta\sin\theta - \tilde{u}_{\ell\theta}\sin\ell\theta\cos\theta \tag{7.2b}$$

and

$$u_z = \tilde{u}_{\ell z}\cos\ell\theta. \tag{7.2c}$$

8. Lamb dipoles

Of the nine possible point dipoles which may act within a continuous space, the explicit formulae for Lamb's problem allow obtaining a subset of these, namely the solutions for the six dipoles acting at the surface of the half-space which do not depend on derivatives of the displacement functions with respect to the vertical direction, see figure 2. When expressed in cylindrical coordinates, these six dipoles can be written as follows. Let u, v and w be a shorthand for the response functions owing to a horizontal load (i.e. $u \equiv \tilde{u}_{1r}, v \equiv \tilde{u}_{1\theta}$ and $w \equiv \tilde{u}_{1z}$ in equation (7.1)) and U and W are the response functions owing to a vertical load (i.e. $U \equiv \tilde{u}_{0r}, W \equiv \tilde{u}_{0z}$). Then [9]:

$$\begin{aligned}\mathbf{G}_{xx} = -\frac{1}{2}\Bigg\{&\left(\frac{\partial u}{\partial r} + \frac{u-v}{r}\right)\hat{\mathbf{r}} + \left(\frac{\partial w}{\partial r} + \frac{w}{r}\right)\hat{\mathbf{k}} + \left(\frac{\partial u}{\partial r} - \frac{u-v}{r}\right)\cos 2\theta\hat{\mathbf{r}} \\ &- \left(\frac{\partial v}{\partial r} + \frac{u-v}{r}\right)\sin 2\theta\hat{\mathbf{t}} + \left(\frac{\partial w}{\partial r} - \frac{w}{r}\right)\cos 2\theta\hat{\mathbf{k}}\Bigg\},\end{aligned} \tag{8.1a}$$

$$\mathbf{G}_{yy} = -\frac{1}{2}\left\{\left(\frac{\partial u}{\partial r} + \frac{u-v}{r}\right)\hat{\mathbf{r}} + \left(\frac{\partial w}{\partial r} + \frac{w}{r}\right)\hat{\mathbf{k}} - \left(\frac{\partial u}{\partial r} - \frac{u-v}{r}\right)\cos 2\theta\hat{\mathbf{r}} + \left(\frac{\partial v}{\partial r} + \frac{u-v}{r}\right)\sin 2\theta\hat{\mathbf{t}} - \left(\frac{\partial w}{\partial r} - \frac{w}{r}\right)\cos 2\theta\hat{\mathbf{k}}\right\}, \tag{8.1b}$$

$$\mathbf{G}_{xy} = -\frac{1}{2}\left\{-\left(\frac{\partial v}{\partial r} - \frac{u-v}{r}\right)\hat{\mathbf{t}} + \left(\frac{\partial u}{\partial r} - \frac{u-v}{r}\right)\hat{\mathbf{r}}\sin 2\theta + \left(\frac{\partial v}{\partial r} + \frac{u-v}{r}\right)\cos 2\theta\hat{\mathbf{t}} + \left(\frac{\partial w}{\partial r} - \frac{w}{r}\right)\sin 2\theta\hat{\mathbf{k}}\right\}, \tag{8.1c}$$

$$\mathbf{G}_{yx} = -\frac{1}{2}\left\{\left(\frac{\partial v}{\partial r} - \frac{u-v}{r}\right)\hat{\mathbf{t}} + \left(\frac{\partial u}{\partial r} - \frac{u-v}{r}\right)\hat{\mathbf{r}}\sin 2\theta + \left(\frac{\partial v}{\partial r} + \frac{u-v}{r}\right)\cos 2\theta\hat{\mathbf{t}} + \left(\frac{\partial w}{\partial r} - \frac{w}{r}\right)\sin 2\theta\hat{\mathbf{k}}\right\}, \tag{8.1d}$$

$$\mathbf{G}_{zx} = -\left\{\frac{\partial U}{\partial r}\cos\theta\hat{\mathbf{r}} - \frac{U}{r}\sin\theta\hat{\mathbf{t}} + \frac{\partial W}{\partial r}\cos\theta\hat{\mathbf{k}}\right\} \tag{8.1e}$$

and

$$\mathbf{G}_{zy} = -\left\{\frac{\partial U}{\partial r}\sin\theta\hat{\mathbf{r}} + \frac{U}{r}\cos\theta\hat{\mathbf{t}} + \frac{\partial W}{\partial r}\sin\theta\hat{\mathbf{k}}\right\}, \tag{8.1f}$$

where $\hat{\mathbf{r}}, \hat{\mathbf{t}}, \hat{\mathbf{k}}$ are unit vectors in the radial, tangential and vertical directions, respectively. The $\mathbf{G}_{xx}$ and $\mathbf{G}_{yy}$ are the response functions for cracks while the other functions are for single couples, with the first index identifying the direction of the forces in the couple and the second index the direction of the moment arm, see figure 2. From the above, we can readily infer also the expressions for a double couple lying in the horizontal plane on the surface (seismic moment) as well as for a torsional moment with vertical axis, namely

$$\begin{aligned}\mathbf{M}_z &= \mathbf{G}_{yx} + \mathbf{G}_{xy} \\ &= -\left\{\left(\frac{\partial u}{\partial r} - \frac{u-v}{r}\right)\hat{\mathbf{r}}\sin 2\theta + \left(\frac{\partial v}{\partial r} + \frac{u-v}{r}\right)\cos 2\theta\hat{\mathbf{t}} + \left(\frac{\partial w}{\partial r} - \frac{w}{r}\right)\sin 2\theta\hat{\mathbf{k}}\right\}\end{aligned} \tag{8.2}$$

and

$$\mathbf{T}_z = \frac{1}{2}(\mathbf{G}_{yx} - \mathbf{G}_{xy}) = -\frac{1}{2}\left(\frac{\partial v}{\partial r} - \frac{u-v}{r}\right)\hat{\mathbf{t}}. \tag{8.3}$$

All of the above solutions for dipoles involve derivatives with respect to the range r, and all of Lamb's formulae contain terms of the form

$$F(r,\tau) = \frac{1}{r}f(\tau), \quad \tau = \tau(t,r) = \frac{C_S t}{r}, \quad \frac{\partial f(\tau)}{\partial r} = \frac{\partial f(\tau)}{\partial \tau}\frac{\partial \tau}{\partial r} = (-)\frac{\tau}{r}\frac{\partial f(\tau)}{\partial \tau},$$

which implies

$$\frac{\partial F}{\partial r} = \frac{\partial(\frac{1}{r}f)}{\partial r} = (-)\frac{1}{r^2}\left(f + \tau\frac{\partial f}{\partial \tau}\right). \tag{8.4}$$

This leads to the following derivatives of interest:

$$f = 1, \quad \frac{\partial(1/r)}{\partial r} = (-)\frac{1}{r^2} \tag{8.5a}$$

$$f = \tau^2, \quad \frac{\partial((1/r)\tau^2)}{\partial r} = (-)\frac{3\tau^2}{r^2} \tag{8.5b}$$

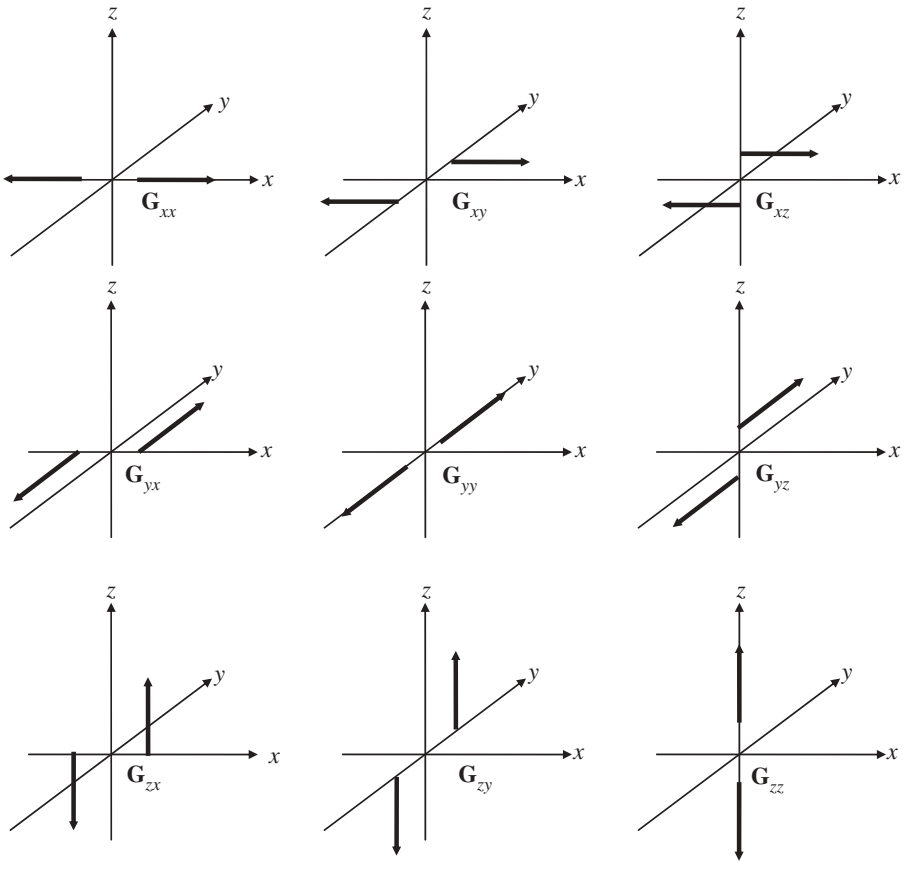

Figure 2. The nine dipoles. Of these, only the six in the left and centre columns can be evaluated with Lamb's formulae.

$$f=\sqrt{\tau^2-\kappa_j^2},\quad \frac{\partial(1/r)\sqrt{\tau^2-\kappa_j^2}}{\partial r}=(-)\frac{1}{r^2}\frac{2\tau^2-\kappa_j^2}{\sqrt{\tau^2-\kappa_j^2}} \tag{8.5c}$$

$$f=\sqrt{\kappa_j^2-\tau^2},\quad \frac{\partial(1/r)\sqrt{\kappa_j^2-\tau^2}}{\partial r}=\frac{1}{r^2}\frac{2\tau^2-\kappa_j^2}{\sqrt{\kappa_j^2-\tau^2}} \tag{8.5d}$$

$$f=\frac{1}{\sqrt{\tau^2-\kappa_j^2}},\quad \frac{\partial}{\partial r}\left(\frac{1}{r\sqrt{\tau^2-\kappa_j^2}}\right)=\frac{\kappa_j^2}{r^2(\tau^2-\kappa_j^2)^{3/2}} \tag{8.5e}$$

and

$$f=\frac{1}{\sqrt{\kappa_j^2-\tau^2}},\quad \frac{\partial}{\partial r}\left(\frac{1}{r\sqrt{\kappa_j^2-\tau^2}}\right)=(-)\frac{\kappa_j^2}{r^2(\kappa_j^2-\tau^2)^{3/2}}. \tag{8.5f}$$

These derivatives are valid whether the roots κ_j are either real or complex.

On the other hand, in §6, we made reference to three discontinuities in the (dimensionless) time domain τ (equations (6.3) and (6.5)), which in the current notation are

$$\Delta u|_{\tau=\gamma}=\frac{1}{2\pi\mu r},\quad \Delta v|_{\tau=1}=\frac{1}{2\pi\mu r},\quad \Delta W|_{\tau=\gamma}=\frac{1-\nu}{2\pi\mu r}. \tag{8.6}$$

Since the partial derivatives in the dipoles are with respect to r and not τ, then the above discontinuities lead to the singularities

$$\left.\frac{\partial u}{\partial r}\right|_{\tau=\gamma} = \left.\frac{\partial u}{\partial \tau}\frac{\partial \tau}{\partial r}\right|_{\tau=\gamma} = (-)\frac{\tau}{r}\left.\frac{\partial u}{\partial \tau}\right|_{\tau=\gamma} = (-)\frac{\gamma}{2\pi\mu r^2}\delta(\tau-\gamma), \tag{8.7a}$$

$$\left.\frac{\partial v}{\partial r}\right|_{\tau=1} = \left.\frac{\partial v}{\partial \tau}\frac{\partial \tau}{\partial r}\right|_{\tau=1} = (-)\frac{\tau}{r}\left.\frac{\partial v}{\partial \tau}\right|_{\tau=1} = (-)\frac{1}{2\pi\mu r^2}\delta(\tau-1) \tag{8.7b}$$

and

$$\left.\frac{\partial W}{\partial r}\right|_{\tau=\gamma} = \left.\frac{\partial W}{\partial \tau}\frac{\partial \tau}{\partial r}\right|_{\tau=\gamma} = (-)\frac{\tau}{r}\left.\frac{\partial W}{\partial \tau}\right|_{\tau=\gamma} = (-)(1-\nu)\frac{\gamma}{2\pi\mu r^2}\delta(\tau-\gamma). \tag{8.7c}$$

Taking these singularities into account, then the terms of interest which appear in the various dipoles are as follows:

$$\frac{u-v}{r} = \frac{1}{2\pi\mu r^2}\begin{cases} \frac{1}{2}(1-\nu)\left[\sum_{j=1}^{3} C_j \dfrac{2\tau^2-\kappa_j^2}{\sqrt{\tau^2-\kappa_j^2}} - 1\right], & a<\tau<1, \\ \nu + (1-\nu)C_1\dfrac{2\tau^2-\gamma^2}{\sqrt{\tau^2-\gamma^2}}, & 1<\tau<\gamma, \\ \nu, & \tau>\gamma, \end{cases} \tag{8.8a}$$

$$\frac{\partial u}{\partial r} = (-)\frac{1}{2\pi\mu r^2}\begin{cases} \frac{1}{2}(1-\nu)\tau^2\sum_{j=1}^{3} C_j \dfrac{2\tau^2-3\kappa_j^2}{(\tau^2-\kappa_j^2)^{3/2}} & a<\tau<1, \\ 1+(1-\nu)\tau^2 C_1\dfrac{(2\tau^2-3\gamma^2)}{(\tau^2-\gamma^2)^{3/2}} & 1\le\tau<\gamma, \\ 1+\gamma\delta(\tau-\gamma) & \tau\ge\gamma, \end{cases} \tag{8.8b}$$

$$\frac{\partial v}{\partial r} = (-)\frac{1}{2\pi\mu r^2}\begin{cases} \frac{1}{2}(1-\nu)\left[1-\sum_{j=1}^{3} C_j \dfrac{2\tau^2-\kappa_j^2}{\sqrt{\tau^2-\kappa_j^2}}\right], & a<\tau<1, \\ (1-\nu)\left[1-C_1\dfrac{2\tau^2-\gamma^2}{\sqrt{\tau^2-\gamma^2}}\right]+\delta(\tau-1), & 1\le\tau<\gamma, \\ 1-\nu, & \tau\ge\gamma, \end{cases} \tag{8.8c}$$

$$\frac{\partial W}{\partial r} = (-)\frac{(1-\nu)}{2\pi\mu r^2}\begin{cases} \frac{1}{2}\left(1+\sum_{j=1}^{3}\dfrac{A_j\kappa_j^2}{(\tau^2-\kappa_j^2)^{3/2}}\right), & a<\tau<1, \\ 1+\dfrac{A_1\gamma^2}{(\tau^2-\gamma^2)^{3/2}}, & 1\le\tau<\gamma, \\ 1+\gamma\delta(\tau-\gamma), & \tau\ge\gamma \end{cases} \tag{8.8d}$$

and

$$\frac{\partial w}{\partial r} = -\frac{\partial U}{\partial r} = \text{complicated}. \tag{8.8e}$$

We omitted the last derivative in equation (8.8*e*) above because it is rather cumbersome, inasmuch as it involves derivatives of the elliptical functions in which τ appears as argument in the modulus n and n^{-1}, see equations (4.4 and 4.5). Nonetheless, these too could be written down in terms of explicit formulae without much problem, a task that is left to the readers to carry out.

To illustrate matters, consider the case of a torsional dipole. From equations (8.3), (8.8*a*) and (8.8*c*), we readily obtain

$$u_\theta = \frac{1}{4\pi\mu r^2}\{\mathcal{H}(\tau-1)+\delta(\tau-1)\}, \tag{8.9}$$

which agrees perfectly with the exact solution obtained by the method of images [9, pp. 83–85].

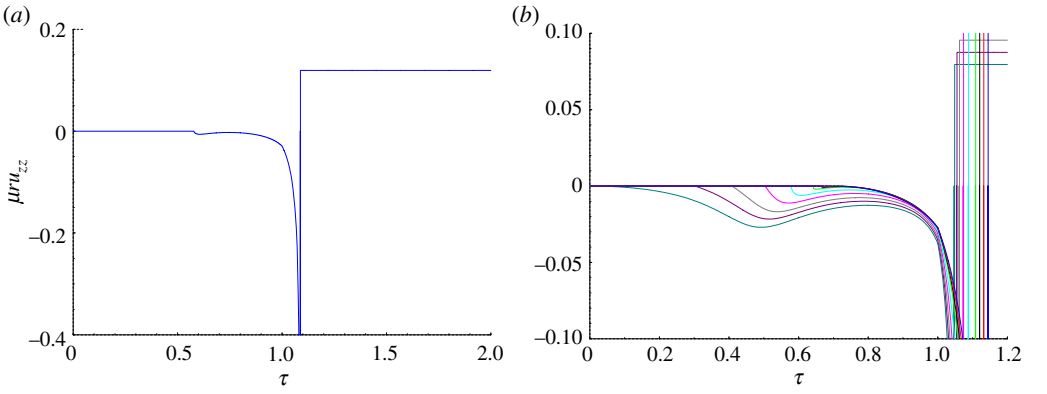

Figure 3. Vertical displacement due to vertical point (step) load. (*a*) Response for Poisson's ratio $\nu = 0.25$. (*b*) Detail for $\nu = 0$, 0.05, 0.10, 0.15, 0.25, 0.33, 0.40, 0.45, 0.50. Increasing values of this ratio correspond to curves lying closer to the origin. (Online version in colour.)

9. Graphic illustration

Figures 3–6 depict in their upper part a global view of the response functions given by equations (4.1)–(4.4) for the classical Pekeris–Chao case of $\nu = 0.25$, $\mu = C_S = r = 1$, and then underneath a blow-up of the corresponding response function for a full set of Poisson's ratios in the range from 0 to 0.5, which reveal the detail of the various wave arrivals together with their abrupt transitions. Thereafter, figure 7 shows the displacements along the vertical axis below the load. All of these agree perfectly with the known results. Observe that the plots for the response functions due to a horizontal load do *not* include the implicit factors $(\cos\theta)$ and $(-\sin\theta)$ factors, which must be added to obtain the actual variation with the azimuth.

Interested readers can download the electronic supplementary material to this article containing the detailed mathematical proof of the formulae presented herein, and also a brief Matlab program which evaluates all of the components and for any Poisson's ratio.

10. Whither Q_1?

Cognoscenti will surely have noticed that the response functions given herein are free from cumbersome terms involving the complex poles Q_1 and Q_2 which arise in contour integrals on the unit circle when the roots are complex [4,9]. Such integrals have the form

$$I = \frac{2}{\pi}\int_0^{(1/2)\pi} \frac{C\,\mathrm{d}\theta}{C + D\sin^2\theta} = \frac{4Z}{(Q_2 - Q_1)}, \quad Z = \frac{C}{D}, \quad Q_1 Q_2 = 1, \quad |Q_1| < 1, \tag{10.1}$$

where C is complex and D is real and non-negative. The Q_1 and Q_2 terms on the right-hand side satisfy the equation

$$Q_{1,2} = 1 + 2Z \mp 2\sqrt{Z(Z+1)}, \tag{10.2}$$

where the square root term $\sqrt{Z(Z+1)}$ corresponds to Richards' CROOT variable as given by his equation (5.3). It can be shown (see the electronic supplementary material) that Q_1 can be obtained *explicitly* from the equation

$$Q_1 = 1 + 2Z - 2\sqrt{Z(Z+1)}\,\mathrm{sgn}[1 + 2\mathrm{Re}(Z)], \tag{10.3}$$

in which case

$$Q_2 - Q_1 = Q_1^{-1} - Q_1 = 4\sqrt{Z(Z+1)}\,\mathrm{sgn}[1 + 2\mathrm{Re}(Z)]. \tag{10.4}$$

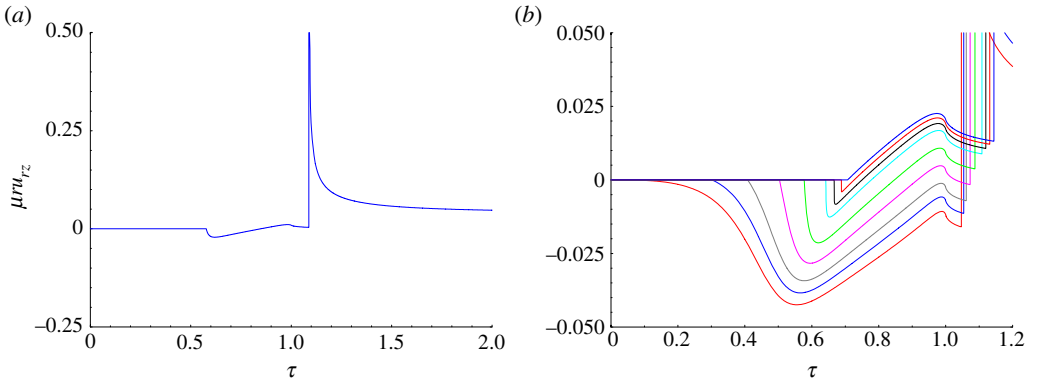

Figure 4. Radial displacement due to vertical point (step) load. (*a*) Response for Poisson's ratio $\nu = 0.25$. (*b*) Detail for $\nu = 0$, 0.05, 0.10, 0.15, 0.25, 0.33, 0.40, 0.45, 0.50. Increasing values of this ratio correspond to curves lying closer to the origin. (Online version in colour.)

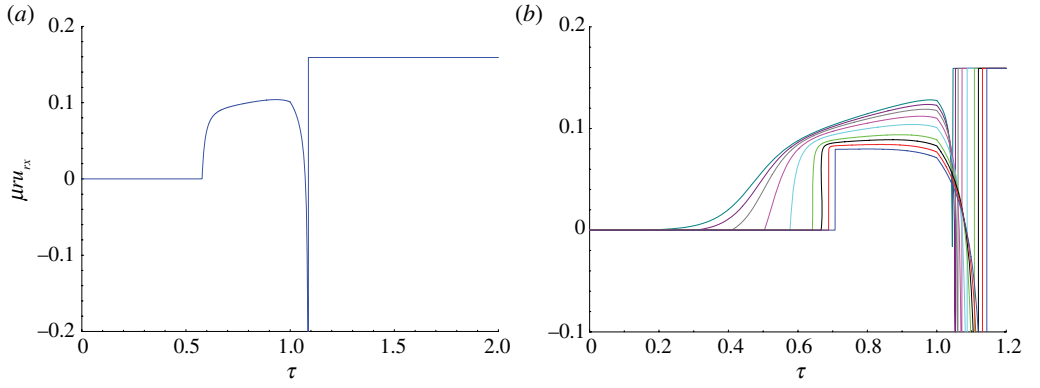

Figure 5. Radial displacement due to horizontal point (step) load. (*a*) Response for Poisson's ratio $\nu = 0.25$. (*b*) Detail for $\nu = 0$, 0.05, 0.10, 0.15, 0.25, 0.33, 0.40, 0.45, 0.50. Increasing values of this ratio correspond to curves lying closer to the origin. A factor $(\cos\theta)$ is implied. (Online version in colour.)

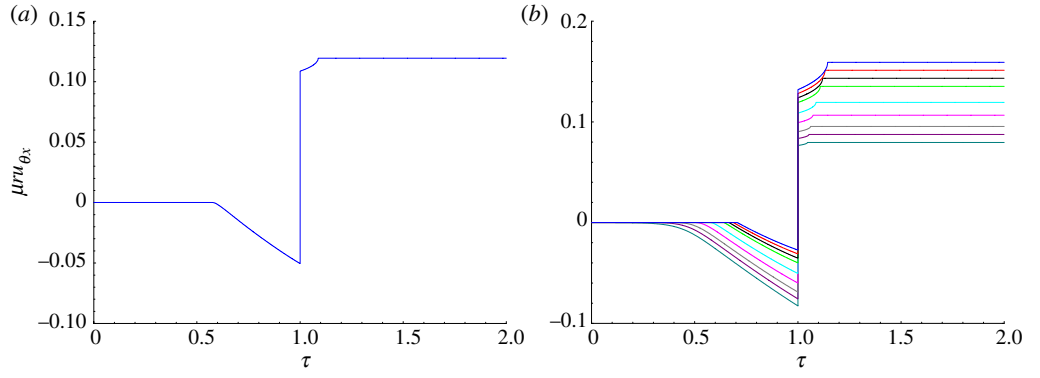

Figure 6. Tangential displacement due to horizontal point (step) load. (*a*) Response for Poisson's ratio $\nu = 0.25$. (*b*) Detail for $\nu = 0$, 0.05, 0.10, 0.15, 0.25, 0.33, 0.40, 0.45, 0.50. Increasing values of this ratio correspond to curves that lie lower, but the magnitude of the jump at $\tau = 1$ does not depend on Poisson's ratio. A factor $(-\sin\theta)$ is implied. (Online version in colour.)

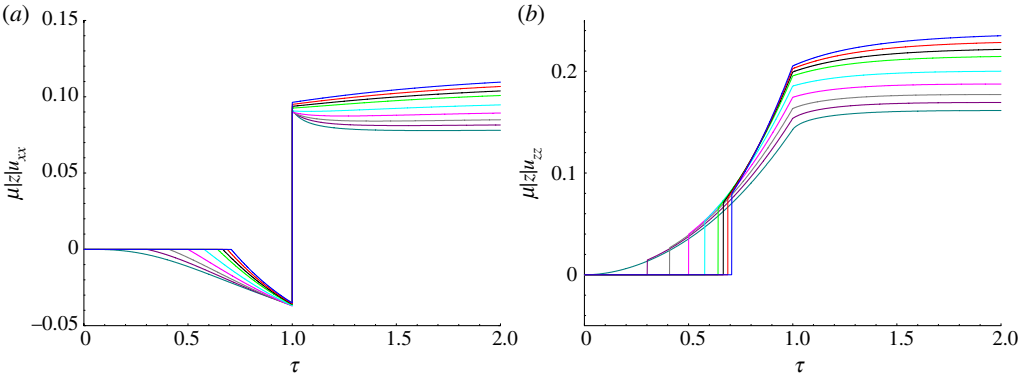

Figure 7. Response at depth $d = |z|$ below point load for $\nu = 0, 0.05, 0.10, 0.15, 0.25, 0.33, 0.40, 0.45, 0.50$. (*a*) Horizontal load. (*b*) Vertical load. Here, $\tau = tC_S/|z|$. Increases in Poisson's ratio result in curves that lie lower and/or closer to the origin. (Online version in colour.)

It can also be shown that

$$\frac{Z}{\sqrt{Z(Z+1)}} = \frac{Z}{\sqrt{Z}\sqrt{Z+1}}\mathrm{sgn}[1+2\mathrm{Re}(Z)] = \frac{\sqrt{Z}}{\sqrt{Z+1}}\mathrm{sgn}[1+2\mathrm{Re}(Z)]. \tag{10.5}$$

Combination of both of the above yields finally

$$I = \frac{4Z}{(Q_2 - Q_1)} = \frac{\sqrt{Z}}{\sqrt{Z+1}}, \tag{10.6}$$

which has *exactly the same form* as the solution for purely real coefficients C, D. Observe that the final ratio on the right-hand side is free from any numerical tests, such as the requirement for the absolute value of some quantity, say $|Q_1| < 1$, and indeed, *these quantities need not be evaluated in the first place*. Hence, exactly the same formulae apply to both real and complex roots. This is a significant improvement because it allows rendering all of the response functions in a much simpler, common form, and especially so concerning the variation with time. For example, compare below the classical treatment of complex roots on the left-hand side [4] versus the current form on the right-hand side:

$$\frac{1}{(\tau^2 - a^2)[Q_2(\tau) - Q_1(\tau)]} \quad \text{versus} \quad \frac{1}{\sqrt{\tau^2 - \kappa_j^2}}. \tag{10.7}$$

Thus, only one set of functions is needed instead of two, and these are also readily amenable to further manipulations, such as taking derivatives to obtain explicit expressions for dipoles or for impulsive loads, as presented earlier. This is a significant advantage in our formulation which ultimately emanates from the lack of need to distinguish between real and complex roots.

11. Conclusions

This paper revisited Lamb's problem of a suddenly applied, horizontal and vertical point load applied at the surface of an elastic, homogeneous half-space of arbitrary Poisson's ratio. It presented a compact set of explicit space–time formulae for the following problems:

— All response functions for receivers placed at the surface of the half-space.
— All response functions for receivers placed at depth underneath the load, i.e. along the epicentral axis.
— Out of nine possible dipoles, explicit formulae are also given for the six dipoles which correspond to horizontal cracks and horizontally polarized single couples.

We also demonstrated that the integrals associated with complex roots of the Rayleigh function attain exactly the same form as those for the real roots. This allowed us to provide a unique set of formulae that is valid for any arbitrary Poisson's ratio, which simplified in turn the task of taking spatial and temporal derivatives needed for dipoles.

We wish to thank Dr Paul G. Richards for openly reviewing an initial version of this paper and bringing to our attention his own, much earlier contribution to the subject matter. A careful cross-check ultimately demonstrated a complete agreement between our formulae for displacements, except for trivial changes in signs due to the different coordinate conventions employed by each of us. Readers should also be alerted to the fact that Richards' formula for a vertical load (his I_3) differs substantially from our equation (4.1) as well as from the classical formulae found in either Mooney [4] or Eringen & Suhubi [10], which at first seemed to suggest to us that it might be incorrect. However, after carrying out some additional mathematical transformations with the aid of the Rayleigh function, we succeeded in demonstrating that our formulae were fully equivalent and thus constitute nothing but alternative mathematical realizations of one and the same response function.

References

1. Lamb H. 1904 On the propagation of tremors over the surface of an elastic solid. *Phil. Trans. R. Soc. Lond. A* **203**, 1–42. (doi:10.1098/rsta.1904.0013)
2. Pekeris CL. 1955 The seismic surface pulse. *Proc. Natl Acad. Sci. USA* **41**, 469–480. (doi:10.1073/pnas.41.7.469)
3. Chao CC. 1960 Dynamical response of an elastic half-space to tangential surface loadings. *J. Appl. Mech.* ASME **27**, 559–567. (doi:10.1115/1.3644041)
4. Mooney HM. 1974 Some numerical solutions for Lamb's problem. *Bull. Seismol. Soc. Am.* **64**, 473–491.
5. Aki K, Richards PG. 2002 *Quantitative seismology*, 2nd edn. Mill Valley, CA: University Science Books.
6. Cerruti V. 1882 *Ricerche intorno all'equilibrio dei corpi elastici isotropi*, vol. 13. Rome, Italy: Reale Accademia dei Lincei.
7. Boussinesq VJ. 1885 *Application des potentiels a l'étude de l'équilibre et du movement des solides élastiques*. Paris, France: Gauthier-Villars, Imprimeur-Libraire.
8. Richards PG. 1979 Elementary solutions to Lamb's problem for a point source and their relevance to three-dimensional studies of spontaneous crack propagation. *Bull. Seismol. Soc. Am.* **69**, 947–956.
9. Kausel E. 2006 *Fundamental solutions in elastodynamics: a compendium*. Cambridge, UK: Cambridge University Press.
10. Eringen AC, Suhubi ES. 1975 *Elastodynamics*, vol. II (Linear Theory). New York, NY: Academic Press.